The structure of a complex of human 17β-hydroxysteroid dehydrogenase with estradiol and NADP+ identifies two principal targets for the design of inhibitors

Rock Breton†, Dominique Housset, Catherine Mazza and Juan Carlos Fontecilla-Camps*

Background: The steroid hormone 17β-estradiol is important in the genesis and development of human breast cancer. Its intracellular concentration is regulated by 17β-hydroxysteroid dehydrogenase, which catalyzes the reversible reduction of estrone to 17β-estradiol. This enzyme is thus an important target for inhibitor design. The precise localization and orientation of the substrate and cofactor in the active site is of paramount importance for the design of such inhibitors, and for an understanding of the catalytic mechanism.

Results: The structure of recombinant human 17β-hydroxysteroid dehydrogenase of type 1 (17β-HSD1) in complex with estradiol at room temperature has been determined at 1.7 Å resolution, and a ternary 17β-HSD1–estradiol–$NADP^+$ complex at –150°C has been solved and refined at 2.20 Å resolution. The structures show that estradiol interacts with the enzyme through three hydrogen bonds (involving side chains of Ser142, Tyr155 and His221), and hydrophobic interactions between the core of the steroid and nine other residues. The $NADP^+$ molecule binds in an extended conformation, with the nicotinamide ring close to the estradiol molecule.

Conclusions: From the structure of the complex of the enzyme with the substrate and cofactor of the oxidation reaction, the orientation of the substrates for the reduction reaction can be deduced with confidence. A triangular hydrogen-bond network between Tyr155, Ser142 and O17 from estradiol probably facilitates the deprotonation of the reactive tyrosine, while the conserved Lys159 appears not to be directly involved in catalysis. Both the steroid-binding site and the NADPH-binding site can be proposed as targets for the design of inhibitors.

Address: Laboratoire de Cristallographie et Cristallogenèse des Protéines, Institut de Biologie Structurale J.-P. Ebel, CEA - CNRS 41, avenue des Martyrs, F-38027 Grenoble cedex, France.

†Present address: Molecular Endocrinology, CHUL Research Center, 2705 boulevard Laurier, Québec, G1V 4G2, Canada.

*Corresponding author.
E-mail: juan@lccp.ibs.fr

Key words: 17β-hydroxysteroid dehydrogenase, complex, estradiol, $NADP^+$, X-ray structure

Received: 15 April 1996
Revisions requested: 8 May 1996
Revisions received: 4 June 1996
Accepted: 18 June 1996

Structure 15 August 1996, 4:905–915

Introduction

It is well known that 17β-estradiol (E2), plays an important role in the genesis and development of human breast cancer [1,2]. 17β-Hydroxysteroid dehydrogenase (17β-HSD) mediates the reversible interconvertion of the biologically inactive estrogen, estrone (E1), to the most active estrogen E2, and thus plays a crucial role in the regulation of intracellular levels of active estrogens in a variety of tissues, including normal and cancerous mammary gland [3–5]. In the endometrium and in hormone-independent human breast cancer cell lines, 17β-HSD activity favours the formation of E1 [6,7]. In contrast, in hormone-dependant cell lines the reductive activity of 17β-HSD, leading to the formation of the most potent estrogen E2 from E1, is predominant [8–11].

The 17β-HSD reaction is catalyzed by five isozymes designated 17β-HSD types 1 to 5 [12,13]. The 17β-HSD type 1 enzyme (17β-HSD1), also referred to as estradiol 17β-dehydrogenase, is a cytosolic protein that almost exclusively catalyzes the reductive reaction (E1→E2) when transiently expressed in cultured mammalian cells [13,14]. A dinucleotide cofactor, either NADPH or NADH, is required for the reaction. Because of its key role in the biosynthesis of active estrogen, this enzyme represents an important target for cancer therapy. A better knowledge of its three-dimensional structure, and especially of those regions involved in specific recognition and binding of steroid substrate, should be instrumental in the design of novel therapeutic agents for the inhibition of estrogen production in the endocrine therapy of breast and other estrogen-sensitive cancers [15].

Primary structure alignments, affinity-labelling studies and site-directed mutagenesis experiments have been used to characterize 17β-HSD1 and to predict the amino acid composition and structure of its active site. The enzyme (MW 34900, 327 residues) belongs to the short-chain alcohol dehydrogenase (SCAD) superfamily [16–18] which can show up to six significantly conserved domains (A–F) identified by multiple sequence alignment. The D domain contains the characteristic Tyr-X-X-X-Lys sequence (Tyr155 and Lys159 in 17β-HSD1) which is conserved in

almost all members of the SCAD superfamily and found to be essential for enzymatic activity [19,20]. The enzyme is active as an homodimer [21]. Several studies have been carried out in order to determine precisely which residues are part of the active site. Chemical modification of specific amino acids suggested that the conserved tyrosine residue may be involved in dimerization of subunits in glucose dehydrogenase [22,23]. However, crystallographic analysis of bacterial 3α,20β-hydroxysteroid dehydrogenase (3α,20β-HSD) and modelling studies with cortisone in the catalytic site [24,25] reveal that the Tyr-X-X-X-Lys sequence along with Ser139 are located in the active site. These residues may promote electrophilic attack of the (C20–O) carbonyl oxygen atom from the cortisone molecule, thus enabling the carbon atom to accept a hydride radical from the reduced cofactor [26]. Site-directed mutagenesis experiments have confirmed the importance of Tyr155 for the activity of human 17β-HSD1 but the lowered catalytic efficiency of the mutant enzyme may also be due to significant changes in its three-dimensional structure, as suggested by the reduced immunoreactivity of the mutant enzyme [27]. Three histidine residues (His210, His213 and His221) of human 17β-HSD1, identified by affinity-labelling studies [28,29] and not conserved in other members of the SCAD superfamily, were also believed to be located near the steroid-binding site and to be involved in hydrogen transfer. However, as recently demonstrated by site-directed mutagenesis experiments, only His221 seems to play a role in steroid binding [27] (CM, unpublished results). This residue is thought to play a structural role as its substitution by either alanine or leucine causes a reduction of immunoreactivity [27] as well as a change in the crystal's symmetry (CM, unpublished results).

Because the precise localization and orientation of the steroid in the active site is of paramount importance for the design of effective and specific inhibitors of human 17β-HSD1, we have co-crystallised the enzyme with its 17β-estradiol substrate and $NADP^+$ and determined the structure of this complex both at room temperature and at low temperature (-150°C). Recombinant 17β-HSD1, overproduced with a baculovirus expression system and purified from *Spodoptera frugiperda* (Sf9) insect cells [30], was used as a source of enzyme.

Recently, the three-dimensional structure of human 17β-HSD1 has been determined independently at 2.20 Å resolution [31]. No density corresponding to the cofactor and the steroid was found although 1 mM $NADP^+$ was present in the crystallization medium. The positions of 17β-estradiol and the $NADP^+$ cofactor were subsequently modelled, the latter being derived from a superposition of the structures of 17β-HSD1 and the 3α,20β-HSD–NAD^+ complex [25]. From these modelling studies, a model for the estrone to estradiol transition state has been proposed. It is clear, however, that only the structure of the ternary complex will furnish a detailed enzyme–substrate interaction at the active site and a putative mechanism description.

This report describes the structures of the 17β-HSD1–estradiol binary complex at 1.7 Å resolution and of the 17β-HSD1–estradiol–$NADP^+$ ternary complex at 2.20 Å resolution. A detailed analysis of the interactions between the enzyme and its substrate and cofactor is presented. Based on our results, a realistic scheme for the catalytic mechanism can be proposed for the reduction reaction.

Results

Overall description of the protein structure

The protein structure does not seem to show any major differences from the model previously published [31]. However, a detailed comparison is not possible as the coordinates for this model are not currently available. As determined by the program DSSP [32], 17β-HSD1 contains seven β strands forming a parallel β sheet and 11 α helices (Table 1). The structure is of the α/β type, including the so-called 'Rossman fold', often encountered in dinucleotide-binding domains (Fig. 1). Moreover, the structure includes two helix-turn-helix motifs (αG″–αG′ and αH′–αH), the latter being involved in dimer formation. No electron density was present for the C-terminal end of the polypeptide chain (residues 288–327), and consequently no model has been built for it. However, mass spectroscopy experiments performed on one of our dissolved crystals showed that all the residues were present (MW 34889 ± 1.5, E Forest, unpublished result). Thus, this part of the chain, which is rich in glycine and alanine residues (19 out of 43), seems to be disordered in the crystal. The packing interactions are very similar to those described by Ghosh *et al.* [31] for the protein alone. Neither the cofactor nor the substrate is involved in interactions with symmetry-related molecules. The main characteristic of the packing is the formation of a crystallographic dimer, thought to be equivalent to the active dimer in solution.

Table 1

Secondary structure elements of 17β-HSD1, as determined by DSSP.

α Helices	Residue range	β Strands	Residue range
		βA	3–7
αB	13–23	βB	30–36
αC	43–51	βC	59–63
αD	69–77	βD	86–89
αE′	104–114		
αE	116–132	βE	135–142
αF	153–173	βF	178–185
αG″	200–206		
αG′	209–229		
αG	233–245	βG	252–254
αH′	260–268		
αH	273–283		

Bold characters indicate the Rossman fold topology.

Figure 1

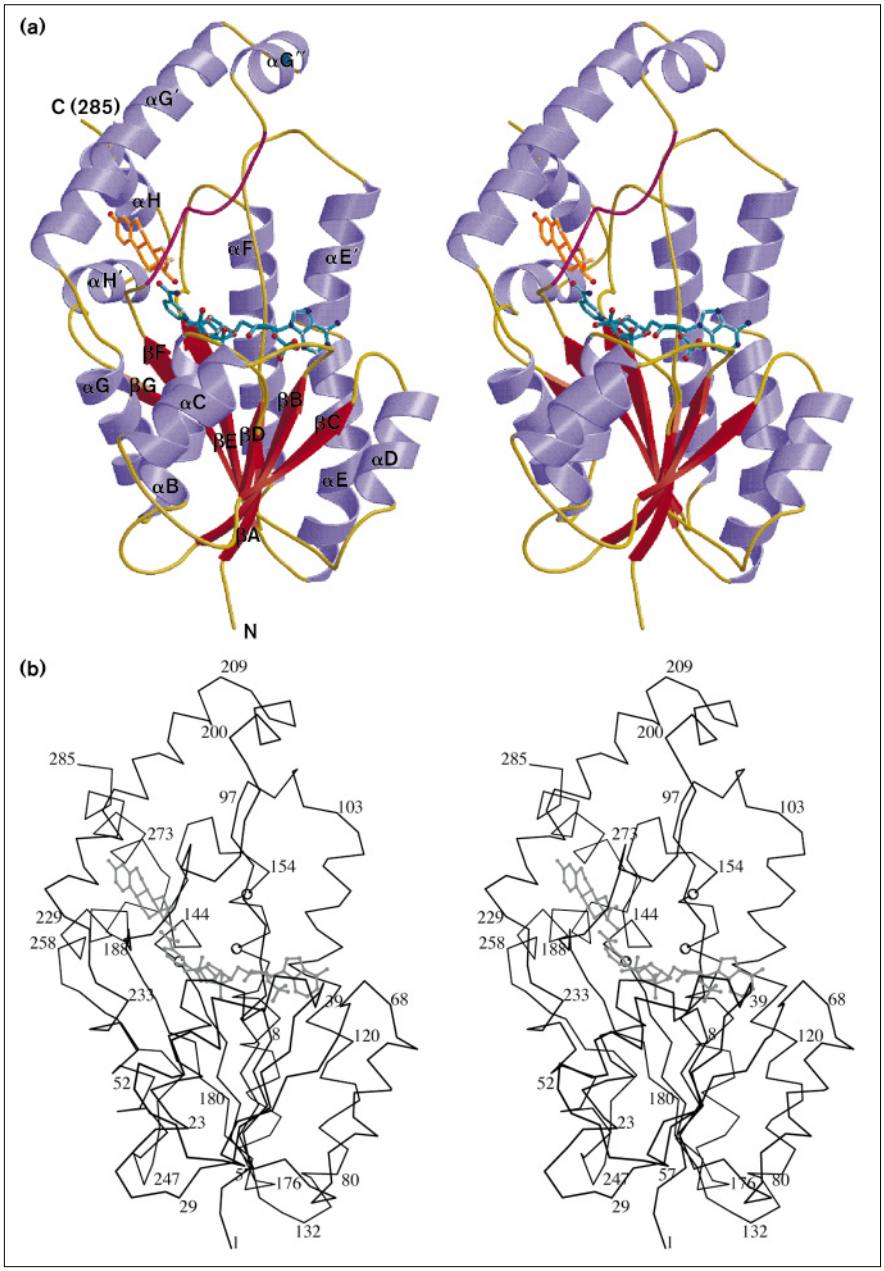

The overall structure of 17β-HSD1–estradiol–NADP$^+$ complex. (a) Stereoscopic view of 17β-HSD1, complexed with estradiol and NADP$^+$. Red arrows represent β strands, α helices are depicted in purple and the rest of the backbone is represented as a yellow coil. Residues 190–197, corresponding to the disordered region, are shown in magenta. The estradiol and NADP$^+$ molecules are depicted as orange and turquoise ball-and-stick models, respectively. (Figure generated with Molscript [51] and Render [52,53]). (b) Stereoscopic view of the Cα backbone, in the same orientation as (a). The substrate and cofactor are shown in grey. Residues implicated in the catalytic mechanism (Ser142, Tyr155 and Lys159) are depicted as circles.

Room temperature model at 1.7 Å resolution

The final room temperature model includes residues 1–285, one estradiol molecule and 127 water molecules. The electron density for estradiol was clearly visible in difference Fourier maps during model building. The structure of estradiol dihydrate, retrieved from the Cambridge database [33], was fitted to the (F_o–F_c) electron-density map and then refined with the rest of the model. The electron-density map is very well defined except for residues 192–198 and the C-terminal end (residues 289–327) which appear to be disordered and were not included in the model. Moreover, five residues (Leu45, Arg67, Arg132, Phe226 and Leu241) were each built with two conformations. The ($2F_o$–F_c) electron-density map corresponding to the steroid is of good quality (Fig. 2). However, its average B factor is significantly higher than for the rest of the model, indicating that the steroid, even if buried in a hydrophobic pocket and stabilized through hydrogen bonds involving hydroxyl groups O3 and O17, could be quite mobile in the crystal structure and the steroid-binding site may not be fully occupied. In addition, the hydroxyl group O17 is located in the proximity of the disordered region (residues 192–198) and points towards a pocket corresponding to the NADP$^+$-binding

Figure 2

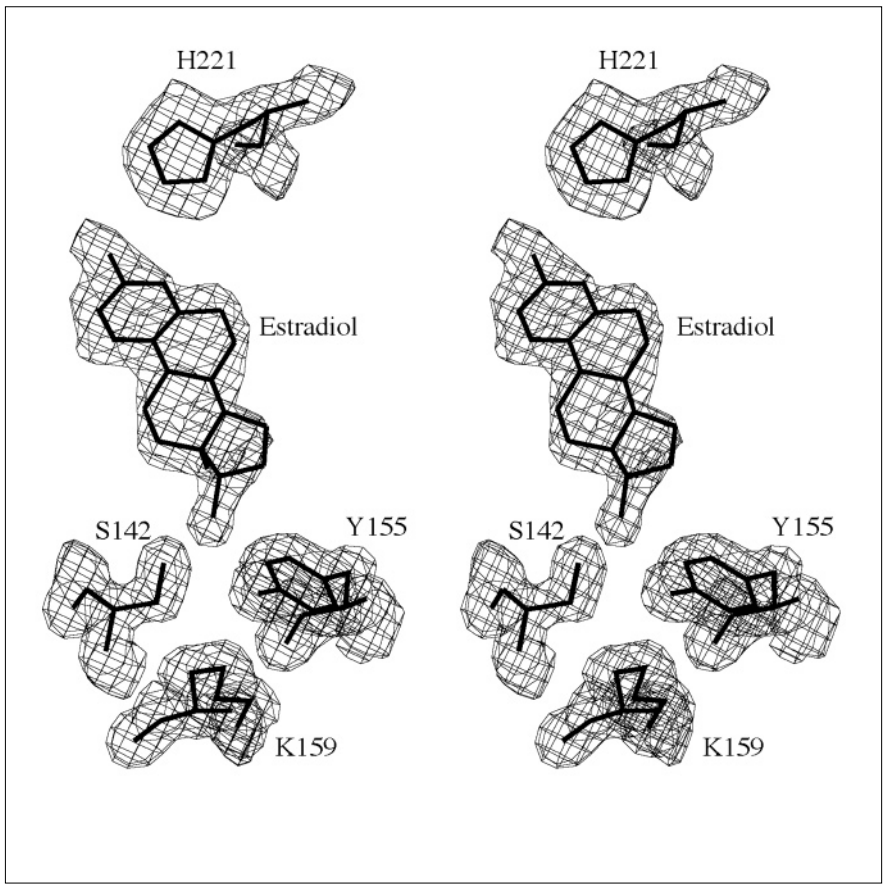

Stereoscopic view of the electron density around the steroid molecule. The $2F_o–F_c$ map, computed with 1.7 Å resolution data, is contoured at the 1σ level.

site. Phe226, modelled with two conformations also points to this region.

Steroid-binding site

The estradiol molecule is located in a pocket formed at the interface of the αG′ helix and the loop between βE and αF. The steroid moiety is mainly stabilized by three hydrogen bonds at its ends: between O3 and Nε2 of His221 (3.14 Å); between O17 and Oγ of Ser142 (3.20 Å); and between O17 and Oη of Tyr155 (3.37 Å). The core of the steroid is maintained with several hydrophobic interactions involving Val143, Met147, Leu149, Pro187, Tyr218, Val225, Phe226, Phe259 and Met279 (Fig. 3). A potential hydrogen bond may occur between the hydroxyl groups of Ser142 and Tyr155 (3.49 Å), forming a triangle-shaped hydrogen-bond network with the O17 hydroxyl group. Moreover, the NH of Gly144 points towards Ser142 Oγ, forming a tight hydrogen bond. Thus, the Ser142 hydroxyl group could serve as a hydrogen donor either to estradiol O17 or to the Tyr155 hydroxyl group.

Low temperature model at 2.2 Å resolution

No major differences were found in the overall protein structure, when the low temperature and room temperature models were compared. The root mean square (rms) difference, calculated for 274 Cα atoms is 0.24 Å. However, for the low temperature model additional electron density was detected in the $NADP^+$ binding region, close to the active site (Fig. 4). Subsequently, it was possible to model the complete dinucleotide. In order to obtain comparable B factors for the residues of the binding pocket (17.6 $Å^2$) and for $NADP^+$ (28.3 $Å^2$), the occupancy of $NADP^+$ had to be set to 0.5. As B factors and occupancies are highly correlated parameters, it is impossible to refine them independently. Thus, this occupancy value is somehow arbitrary, but seems more plausible than assuming large positional fluctuations. This means that, in the crystal, the dinucleotide-binding site may be occupied only half of the time. The nicotinamide ring, and the three phosphate groups have unambiguous matching electron density, while ribose groups are built into less well-defined electron density. The adenine group, exposed to the solvent, could be placed in some reasonable electron density, shared with an alternate conformation of the Arg37 side chain. Moreover, some of the residues of the disordered loop (residues 192–198) in the room temperature model could now be built into the electron density. Residues 192–195 still lack matching electron density, but two plausible conformations have been built

Figure 3

Stereoscopic view of the residues of 17β-HSD1 (light grey) interacting with the estradiol molecule (dark grey). Phe226 is shown with its two modelled conformations.

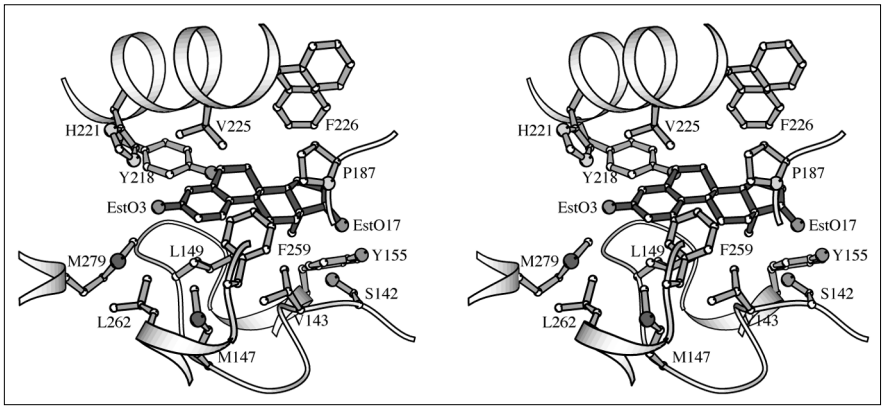

for this part of the polypeptide chain. It appears that the loop may adopt a specific conformation when the $NADP^+$ binds to the enzyme, and may stabilize the nicotinamide ribose group. This phenomenon has already been observed for other $NADP^+$–enzyme complexes [34]. The average B factor is significantly lower for the low temperature structure (Table 2), indicating a reduced mobility of the molecule, particularly in the active site region. Even if the $NADP^+$-binding site may not be fully occupied by the dinucleotide, there is no ambiguity for the interpretation of the

Figure 4

Stereoscopic view of the residual electron-density map around $NADP^+$. The omit F_o–F_c map is computed at 2.2 Å resolution and contoured at the 2.8σ level. The dinucleotide molecule was excluded for the computation of calculated structure factors and phases.

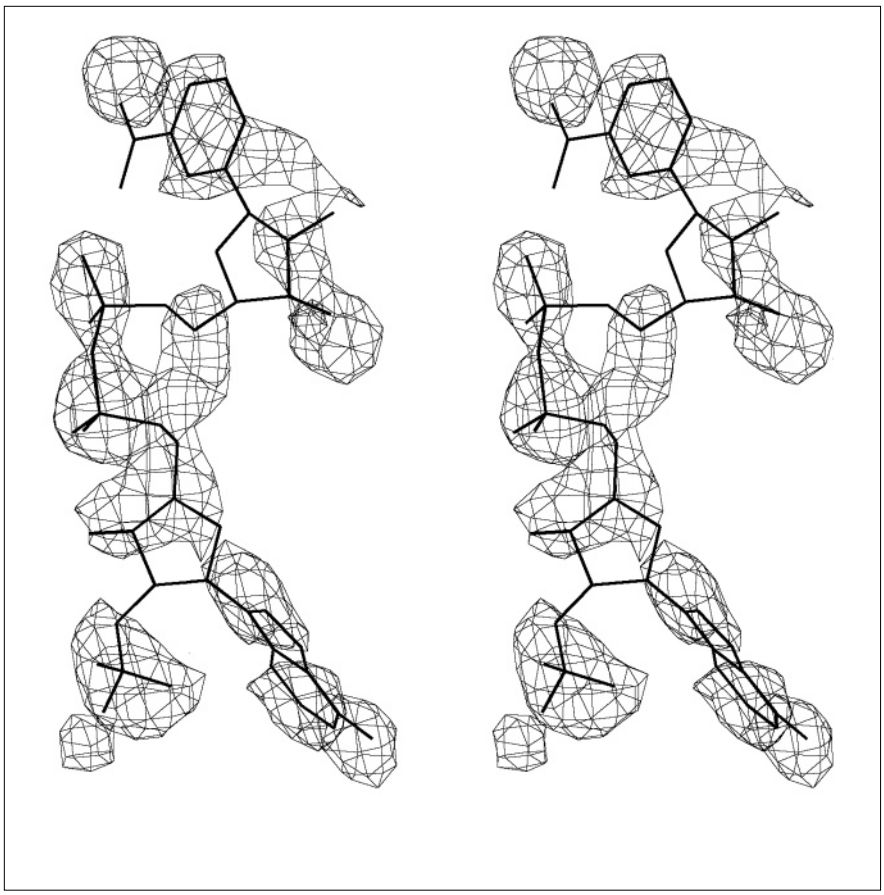

electron density and the relative positions of the three components of the complex are now clearly defined.

NADP$^+$-binding site

The NADP$^+$ molecule binds in an extended conformation, with the nicotinamide moiety pointing towards the active site of the enzyme (Fig. 5). The nicotinamide ring is in a *syn* conformation while the adenine ring is in an *anti* conformation. The B side of the nicotinamide faces the D ring of the steroid, thus allowing the pro-S hydride to be transferred to the latter. The two ribose moieties are C2′-endo puckered, consistent with other short-chain dehydrogenase structures such as dihydropteridine reductase (DHPR) [35,36]. The nicotinamide ring faces the D ring of the steroid, the distance between the nicotinamide C4 atom (hydride donor) and estradiol C17 being 3.62 Å. The major interactions with the protein involve hydrogen bonds with 11 residues (C10, S11, S12, I14, G15, R37, D65, N90, G92, T140, K159, V188 and T190) and hydrophobic contacts with two additional residues (Gly9 and Ala91). In addition, three buried water molecules are hydrogen bonded to the dinucleotide (Fig. 6). The amide nitrogen of Val188 forms a hydrogen bond with the nicotinamide's amide group. The nicotinamide ribose is mainly stabilized through two hydrogen bonds between O2′ and O3′ and the Lys159 Nζ atom, and one hydrogen bond between Thr140 Oγ1 and O5′. The two central phosphate groups hydrogen bond to the main chain NH groups of Ile14 and Gly15 and to Nδ1 of Asn90. The phosphate bound to the adenine ribose is stabilized through three hydrogen bonds formed with the backbone amide groups of Cys10, Ser11 and Arg37, while the ribose itself forms two hydrogen bonds: one between O5′ and Gly92 NH and one between O3′ and the hydroxyl group of Ser11. The adenine, which is fairly exposed to the solvent, only interacts with the side chain of Asp90.

Table 2

Refinement statistics.

	Model at 20°C	Model at –150°C
Model		
Number of residues	285	285
Number of atoms		
protein	2181	2256
estradiol	20	20
NADP$^+$	0	48
solvent	127	142
Data F >2σ(F)		
Resolution (Å)	10.0–1.70	10.0–2.20
Number of reflections	31 798	13 396
Completeness (%)	88.3	84.8
R factor	0.178	0.193
Free R factor	0.203	0.243
Stereochemistry		
Stereochemistry standard deviation from ideality		
bonds (Å)	0.011	0.013
angles (°)	1.72	2.02
improper angles (°)	1.33	1.63
Average B factor (Å^2)		
main chain	22.5	17.8
side chain	25.8	19.3
estradiol	54.8	48.2
NADP$^+$	–	28.3*
solvent	36.7	29.1

*Occupancy set to 0.5 (see text).

Discussion

To our knowledge, this structure constitutes the second published protein–steroid complex three-dimensional X-ray model. The structure shows that the steroid binds through both hydrophobic interactions, concerning the core of the steroid, and three hydrogen bonds at its ends (Fig. 3). The hydrophobic residues essentially protect the four steroid rings from solvent, but do not interact very tightly with the estradiol core. Consequently, the steroid may be able to move slightly in its pocket, as illustrated by its slightly higher B factor values. The hydrogen bonds between O17, and the highly conserved Ser142 and Tyr155 putative catalytic residues (Fig. 6), should be a common feature of 17β-HSD–steroid interactions. On the other hand, the hydrogen bond between O3 and His221 seems to be more specific of steroids with a hydroxyl or a carbonyl group on C3, such as estradiol (a substrate of 17β-HSD1 and 17β-HSD2) or androstenedione (a substrate of 17β-HSD2 and 17β-HSD3). However, the sequence alignment of three 17β-HSD's (types 1 to 3) cannot unambiguously determine the type of residue structurally equivalent to His221 in 17β-HSD1. Puranen *et al.* [27] have shown that the catalytic efficiency of the His221→Ala mutant of 17β-HSD1 was ten to twenty times lower than that of the wild type. Thus, this residue could be a good target to monitor the steroid affinity. Furthermore, a pathway allowing the steroid to enter the binding site is formed by His221, Leu262 and Pro263.

Our structure also sheds light on the catalytic mechanism for the reduction of estrone to estradiol, as the spatial organization of all participants is now completely defined. Consequently, a tentative description of the reaction can be formulated (Fig. 7). A tentative mechanism, based on a sequence alignment and molecular modelling, had previously been proposed concerning the reduction of estrone to estradiol [31]. The present work shows that although some of the elements of this earlier mechanism are basically correct, it is now possible to define the exact role of the implicated residues. The mechanism proposed here is very similar to the one suggested recently for mouse lung carbonyl reductase (MLCR) [37], despite some slight differences in the catalytic serine and tyrosine side chain orientation. The reduction reaction involves a proton and an hydride which are transferred to the estrone molecule. Both Ser142 and Tyr155 could donate a proton to O17.

Figure 5

Stereoscopic close-up view of the active site. Protein residues are show in light grey, estradiol and $NADP^+$ in dark grey. Dashed lines represent hydrogen bonds between estradiol and residues Ser142, Tyr155 and His221. The dotted line illustrates the hydride pathway from the nicotinamide N5 atom to the estradiol C17 atom.

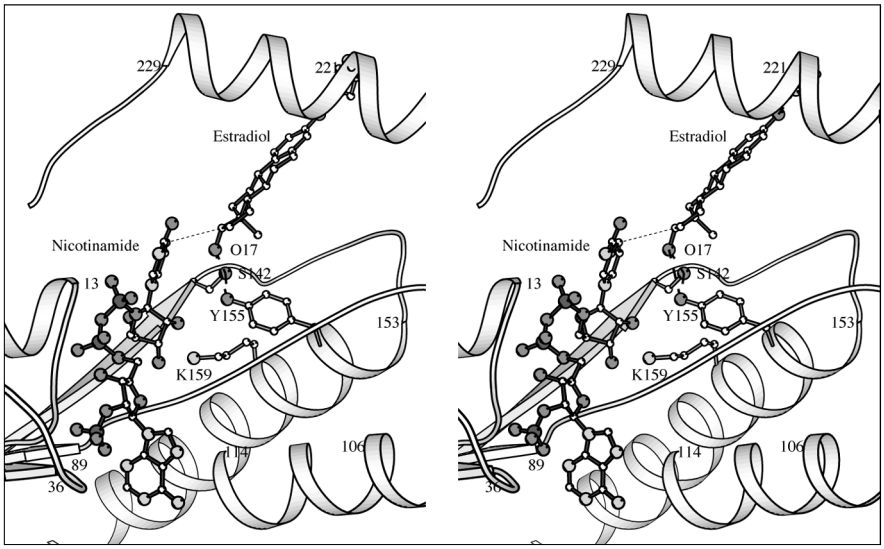

However, due to its lower pK_a, the tyrosine residue seems to be the best candidate. Thus, Ser142 should be able to share its proton with Tyr155, stabilizing the unprotonated state of the tyrosine residue. If Tyr155 is the proton donor, the serine's role may be to lower the apparent pK_a (pK_a^{ap}) of the tyrosine. Located on the other side of the steroid, the nicotinamide liberates the pro-S hydride, 3.62 Å away from C17 (Fig. 5). The optimum pH for the reduction reaction is close to six while the optimum pH for oxidation is between 8 and 10. As the pK_a of tyrosine in water is close to 10.1, the whole environment around Tyr155 should be designed to help its deprotonation. The proximity of hydrophobic residues (possibly including Phe192 from the disordered loop), which shield the active site from the solvent, would certainly reduce the pK_a^{ap}. The exact role of Lys159 also needs to be clarified. Ghosh *et al.* [31] proposed that the side chain of Lys159 could easily move and form a putative hydrogen bond with the hydroxyl group of the tyrosine. Despite the inherent flexibility of this type of residue, no evidence for an enhanced mobility of Lys159 is supported by our crystal structure; the position of this buried side chain is very well defined in electron density and is structurally conserved among other proteins of the SCAD family for which the structures are known (3α,20β-HSD and DHPR). Furthermore, the relative positions of Tyr155 and Lys159, separated by 4.3 Å (distance between the tyrosine hydroxyl group and the lysine Nζ atom), seem to be a constant feature for these enzymes. Thus, the major role of Lys159 could be the stabilization of the dinucleotide through the interaction with the nicotinamide ribose, as for Lys156 in MLCR [37]. Moreover, the presence of five buried water molecules in the neighbourhood of the lysine residue that connect the active site with the protein surface, support the idea that Lys159 is involved in a proton transfer chain.

Although there is now a clear description of the active site, and of the background for the enzymatic reaction, it is not clear which factors could favour the reduction or the oxidation process. 17β-HSD1 is able to catalyze both reactions depending on the pH, while 17β-HSD2 essentially catalyzes the oxidation reaction only [13]. Thus, a sequence alignment of 17β-HSD1 and 17β-HSD2 could shed light on the residues implicated in this reaction. Unfortunately, due to the low level of sequence identity (~23%), an accurate alignment is not available for some regions of the enzyme, including the disordered loop (residues 191–198) and the α helix G′. Thus the role of some residues close to the active site cannot be elucidated at this time. For 17β-HSD1, we can estimate the Tyr155 pK_a^{ap} to fall between six and nine. For both reactions the optimal pH should not be too far from the pK_a^{ap}, in order to make protonation or deprotonation possible. The tyrosine should be protonated for the reduction reaction ($pH \leq pK_a^{ap}$), and able to accept a proton for the oxidation reaction ($pH \geq pK_a^{ap}$).

The structures we have determined also shed some light on the cofactor specificity. It seems that 17β-HSDs, which preferentially catalyse the reduction of their substrates, have higher affinity for $NADP^+$ than for NAD^+ [13,38], but this point has been much debated. 17β-HSD1 lacks the two proximal basic residues which stabilize the 2′-ribose phosphate in NADPH-preferring enzymes. In view of this, and assuming that Leu36 could share the position of the conserved proximal aspartic acid in NADH-preferring enzymes, Tanaka *et al.* [37] proposed that 17β-HSD1 should still be classified as an NADH-preferring enzyme. However, in the structure of 17β-HSD1, the side chain of Leu36 points towards the inside of the enzyme, and is located in an hydrophobic environment made of residues

Figure 6

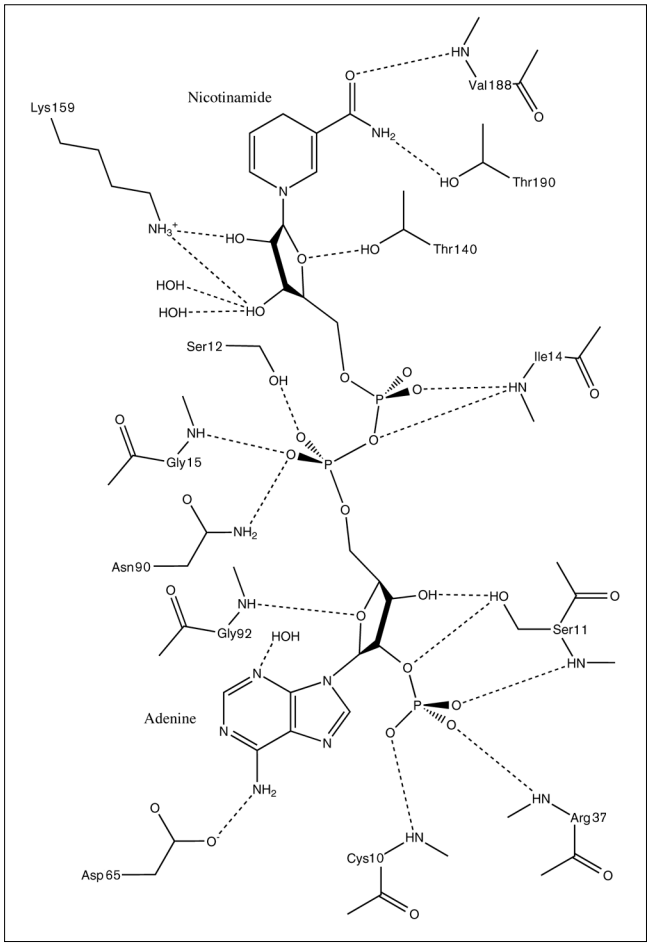

Scheme of interactions between NADP+ and 17β-HSD1, at –150°C. Dashed lines represent hydrogen bonds.

Figure 7

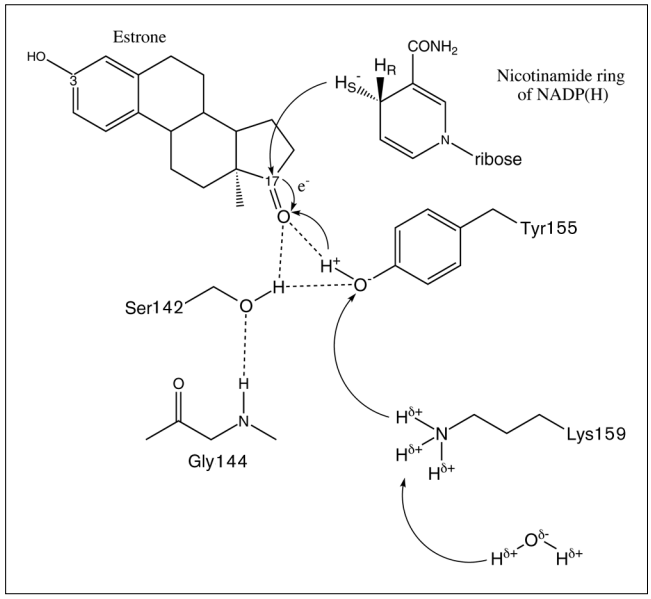

Scheme of the proposed reduction mechanism of estrone to estradiol. Hydrogen bonds are represented with dashed lines. The reaction implies the electrophilic attack of the Tyr155 Oη proton on estradiol O17, and the nucleophilic attack of the nicotinamide pro-S hydride on estradiol C17. Buried water molecules and Lys159 would participate in a proton transfer chain, in order to reprotonate Tyr155.

Cys11 (Cα), Gln42 (Cα), Leu42 (side chain) and Thr61 (Cβ, Cγ2). This is in contrast to the situation in 3α,20β-HSD where the side chain of Asp37 points towards adenosine ribose. Consequently, in 17β-HSD1 the 2′-phosphate is able to approach its binding pocket in which it is mainly stabilized through hydrogen bonds with main chain NH groups of residues Cys10, Ser11 and Arg37. Recently, Luu-The *et al.* [13] have shown that 17β-HSD1 and 17β-HSD3, which catalyze the reduction reaction *in vivo* are NADPH-preferring enzymes, while 17β-HSD2, which catalyzes the oxidation reaction is an NAD+-preferring enzyme. This result is consistent with the sequence alignment of these three enzymes; in 17β-HSD1 and 17β-HSD3 Leu36 is conserved, while 17β-HSD2 has a glutamic acid residue at this position. Mutation experiments on *Drosophila* alcohol dehydrogenase, whose proximal aspartic acid was changed to an asparagine residue, showed a 62-fold increase in NADP+ affinity [39]. Thus, a negatively charged residue like aspartic acid or glutamic acid seems to prevent NADPH binding, whereas a polar or hydrophobic residue at this position allows for it.

On the basis of the structures presented here, two principal targets can be proposed for the design of inhibitors: the steroid-binding site and the dinucleotide-binding site. The binding of an inhibitor in the hydrophobic pocket or to residue His221 would most certainly prevent steroid binding, or at least alter the substrate specificity. Fixing an inhibitor to Ser12 or Lys159 would certainly prevent NADPH binding.

It also appears that the simultaneous modification of Ser142 and Tyr155 abolishes all enzymatic activity. It is not clear, however, whether the modification of just one of them may be enough to keep some residual activity.

Neither His221 nor Tyr155 seem to be essential to preserve the overall structure of the enzyme. Puranen *et al.* [27] have shown that the mutation of either of these residues to alanine leads to the loss of immunoreactivity, as determined by native polyacrylamide gel electrophoresis (PAGE). As these residues are accessible to the solvent, the loss of immunoreactivity could be due to their direct interaction with the antibody. However, the drastic change in side chain volume due to the mutation may cause minor structural modifications in the neighbourhood of these

residues, thus preventing the binding of the antibody. The structure of the ternary complex does not provide any useful clues to establish whether dimerization is necessary for enzymatic activity. The fact that the dimer is formed through an exact crystallographic twofold axis in this space group may abolish some slight differences between the monomers that would enable their cooperativity in solution. Moreover, the exact role and structure of the two disordered regions (residues 192–198 and 286–327) have still to be determined.

Biological implications

17**β**-estradiol is known to be a potent stimulator of human breast cancer. The biosynthesis of this active steroid is catalyzed by the enzyme 17**β**-hydroxysteroid dehydrogenase (17**β**-HSD), which reduces estrone to estradiol. This protein belongs to the short-chain dehydrogenase family of proteins, which share a common fold (termed the Rossman or dinucleotide-binding fold) and an invariant sequence Tyr-X-X-X-Lys, known to be essential for the enzymatic reaction. The structure of several members of this family of enzymes have been recently determined (dihydropterine reductase, 3**α**,20**β**-HSD, 17**β**-HSD1), sheding light on the locations of the catalytic and dinucleotide-binding sites. However, a clear picture of substrate and cofactor binding to 17**β**-HSD1, a necessary step for the design of potential inhibitors and therapeutic agents, was not yet available.

This study presents the high-resolution structure of the ternary complex between the enzyme, the substrate (estradiol) and the cofactor ($NADP^+$). On the basis of this structure, we have been able to precisely describe the steroid- and dinucleotide-binding sites. The nature of the residues implicated in the catalytic reaction (Ser142 and Tyr155), and of those stabilizing the cofactor and the substrate, together with the role of the conserved Lys159 in stabilizing a ribose group of $NADP^+$, are now clearly established. A catalytic mechanism is proposed for the reduction of estrone to estradiol, involving a triangle-shaped hydrogen-bond network between the hydroxyl group of Ser142 and Tyr155, and the steroid O17 atom. The presence of a leucine residue at position 36 (instead of an aspartic acid residue, as is usually encountered for NADH-preferring enzymes) explains the higher affinity of the enzyme for NADPH. This information should be of paramount importance in aiding the design of molecules of therapeutic value that could prevent either substrate or cofactor binding, thus blocking estradiol synthesis.

Materials and methods

Purification of recombinant 17β-HSD

Recombinant 17β-HSD overproduced in a baculovirus expression system was purified with a modification of a previously described procedure [30]. Briefly, infected Sf9 cells were sonicated on ice and unbroken cells and nuclei were pelleted by centrifugation (90 min at 31 400 g). The clear supernatant was diluted approximately two times with a buffer solution containing 40 mM Tris-HCl pH 7.5, 1 mM EDTA, 0.2 mM DTT, and 20% (v/v) glycerol (17β-buffer). The latter was directly loaded on to a Blue-Sepharose CL-6B affinity column, and washed with 80mM NaCl, before stepwise elution with $NADP^+$. Recombinant 17β-HSD1 eluted at about 20 mM $NADP^+$ and resulted in a homogenous preparation.

Crystallization of recombinant 17β-HSD1 in the presence of 17β-estradiol

Crystallization of recombinant 17β-HSD1 was carried out as described for the human placental enzyme [40]. Briefly, the recombinant enzyme concentrated at 10 mg ml^{-1} in the presence of 2 mM β-octylglucoside and 20% glycerol was crystallized in a buffer containing 100 mM HEPES pH 7.5, 100 mM $MgCl_2$ and 24–26% PEG 4000 as precipitant. Under these conditions, 17β-estradiol has very limited solubility (between 25–50 μM) while the 17β-HSD1 concentration used in crystallization (10 mg ml^{-1}) corresponds to a concentration of about 150 mM for the protein dimer (capable of binding 300 mM of 17β-estradiol). In order to obtain the 17β-HSD1–estradiol complex, we slightly changed the crystallization conditions by decreasing the enzyme concentration (from 10 mg ml^{-1} to 4.5 mg ml^{-1}) and increasing the PEG 4000 concentration (from 24 to 32%). At 32% PEG, 500 μM of 17β-estradiol could easily be dissolved corresponding to more than three molecules of steroid per enzyme-binding site. Under these conditions, monoclinic crystals appeared after ten days at room temperature and continued to grow during seven to ten days.

Crystals used for cryocrystallographic experiments were incubated for a few minutes in the same buffer to which 30% (v/v) glycerol was added before the crystals were flashed-cooled under a nitrogen gas stream at –150°C.

Crystals of recombinant 17β-HSD1 were soaked in several heavy-atom containing solutions. Three of these heavy atom reagents gave a small number of significant peaks in the difference Patterson maps. The reagents and soaking conditions are summarized in Table 3.

Data collection and processing

Several native data sets where collected at different temperatures and with different X-ray sources. One data set was collected at room temperature at the W32 synchrotron beam line at LURE (Orsay, France). These data were recorded on an 18 cm diameter Mar Research image plate and processed with MOSFLM (version 5.20) [41] and CCP4 (version 2.12) [42]. Two data sets were collected at low temperature (–150°C). One on the laboratory's Siemens/Xentronics area detector X1000 system, mounted on a Rigaku RU200 rotating-anode X-ray generator, and another one at the D2AM French-CRG synchrotron beam line at the ESRF, using a XRII-CCD detector [43]. Data were processed with XENGEN [44] for the former, and with a modified version of XDS [45,46] for the latter. The data collection statistics are summarized in Table 4. The 17β-HSD1 crystals belong to the monoclinic space group C2. Cell dimensions of room temperature and flash-cooled crystals differ slightly: a=122.33 Å b=44.84 Å c=60.96 Å β=98.84°; and a=122.765 Å b=43.786 Å c=60.528 Å β=99.468°,

Table 3

Soaking solutions of heavy-atom derivatives.

Solution number	Compound	Concentration (mM)	Soaking time (days)
1	$K_2Au(CN)_2$	2	2
2	$K_2Au(CN)_2$	2	5
3	$K_2Pt(CN)_4$	1	2
4	$K_2Pt(NO_2)_4$	0.02	2
5	$K_2Pt(NO_2)_4$	0.02	2

Table 4

Data collection statistics.

Data set	Resolution (Å)	Number of measurements	Number of unique reflections (F >0)	Completeness (%)	λ (Å)	R_{sym}*	R_{merge}†
Lure (20°C)	16.82–1.70	137 576	35 032	97.6	0.900	0.050	
Rigaku (–150°C)	40.0–2.15	29 073	13 157	73.6	1.54	0.058	–
D2AM (–150°C)	40.0–2.15	33 544	12 962	72.5	0.949	0.065	–
Merged data (–150°C)	40.0–2.15	–	15 468	86.5	–	–	0.078

*$R_{sym} = \Sigma_h\Sigma_i|I_{ih} - < I >_h|/(\Sigma_h\Sigma_i < I >_h)$. †$R_{merge} = \Sigma_h\Sigma_i|I_{ih} - < I >_h|/(\Sigma_h\Sigma_i < I >_h)$, the sum is over unique reflections present in both data sets.

respectively. Accordingly, the two data sets could not be merged (R_{merge} > 0.20).

Structure determination

Both molecular replacement (MR) and multiple isomorphous replacement (MIR) methods were used to solve the structure. MR was performed with the Cα backbone model of the 3α,20β-dehydrogenase deposited within the Protein Data Bank (access code 1HSD) [24]. The AMoRe program [47] was used to performed rotation and translation searches. For both rotation and translation functions, the solution with the highest correlation coefficient was the correct one. Unfortunately, the knowledge of Cα atom positions in the unit cell did not provide us with enough phase information to start model building and refinement. Consequently, a derivative search was undertaken. Two heavy-atom salts (Table 3) led to usable derivatives, for which five data sets were collected. Analysis of Patterson difference maps, refinement of heavy atom positions, and calculation of phases were done with the CCP4 suite of programs [42]; the statistics are presented in Table 5. The initial MIR map was improved through solvent-flattening and histogram matching techniques, using DM from the CCP4 suite. Several secondary structure elements could be built in the modified map, and were confirmed by the MR solution. About 40% of the model was built against the first map before the first cycle of refinement. X-PLOR (version 3.1) [48] was then used for refinement, and O [49] and FRODO [50] for model building. In this way the model was updated until completion. Model and MIR phases were combined at the beginning of refinement in order to minimize the bias from the partial model. Two models were refined independently; one using the 1.70 Å resolution data collected at room temperature, and the other using cryogenic data at 2.20 Å resolution. The refinement statistics are presented in Table 2.

Accession numbers

The coordinates of both models have been deposited in the Protein Data bank (entry codes 1FDS and 1FDT).

Acknowledgements

The authors would like to thank J-L Ferrer and M Roth (IBS, Grenoble) for their help using the D2AM ESRF beam line, J-P Benoit and R Fourne for their assistance at LURE (Orsay, France) and E Forest (IBS, Grenoble) for mass spectroscopy measurements. Rock Breton was the recipient of a post-doctoral fellowship from the Medical Research Council (MRC) of Canada.

References

1. Thomas, D.D. (1984). Do hormones cause breast cancer? *Cancer* **53**, 595–601.
2. Lippman, M.E., *et al*., & Gelmann, E. P. (1986). Autocrine and paracrine growth regulation of human breast cancer. *Breast Cancer Res. Treat.* **7**, 59–70.
3. Bonney, R.C., Reed, M.J., Davidson, K., Beranek, P.A. & James, V.H.T. (1983). The relationship between 17β-hydroxysteroid dehydrogenase activity and estrogen concentrations in human breast tumours and in normal breast tissue. *Clin. Endocrinol.* **19**, 727–739.
4. Bonney, R.C., Reed, M.J., Beranek, P.A., Ghilchick, M.W., & James, V.H.T. (1986). Metabolism of [^{3}H] oestradiol *in vivo* by normal breast and tumour tissue in postmenopausal women. *J. Steroid Biochem.* **24**, 361–364.
5. Mehta, R.R. & Das Gupta, T.K. (1993). Regulation of 17β-hydroxysteroid dehydrogenase in a newly-established human breast carcinoma cell line. *J. Steroid Biochem. Mol. Biol.* **46**, 623–629.
6. Schmidt-Gollwitzer, M., Genz, T., Schmidt-Gollwitzer, K., Pollow, B. & Pollow, K. (1978). Correlation between oestradiol and progesterone receptor levels and 17β-hydroxysteroid dehydrogenase activity and endometrial tissue levels of oestradiol, oestrone and progesterone in women. In *Endometrial Cancer.* (Brush, M.G., King, R.J.B. & Taylor, R.W. eds,) pp. 227–241, Bailliere Tindall, London.

Table 5

Data collection and refinement statistics for heavy-atom derivatives.

Solution number	Number of reflections	Resolution (Å)	R_{sym}*(I)	R_{iso}†(F)	R_{cullis}‡	Phasing power	Figure of merit
1	6845	2.95	0.065	0.10	0.66	1.08	–
2	5179	3.10	0.056	0.15	0.72	1.19	–
3	2470	3.80	0.050	0.18	0.82	1.11	–
4	3928	3.60	0.058	0.20	0.65	0.85	–
5	5450	3.20	0.051	0.15	0.69	0.70	–
All	6907	2.95	–	–	–	–	0.47

*$R_{sym} = \Sigma_h\Sigma_i|\ I_{ih} - < I >_h|/(\Sigma_h\Sigma_i < I >_h)$. †$R_{iso} = \Sigma_h|F_{PH} - F_P|/\Sigma_h F_P$. ‡$R_{cullis} = \Sigma_{hcentric}|\ |F_{PH} \pm F_P| - |F_H|/\Sigma_h|F_{PH} \pm F_P|$, with F_{PH}, F_P and F_H structure factors of protein derivative, native protein and heavy atoms alone, respectively.

7. Tseng, L., Mazella, J., Mann, W.J. & Chumas, J. (1982). Estrogen synthesis in normal and malignant human endometrium. *J. Clin. Endocrinol. Metab.* 55, 1029–1031.
8. McNeill, J.M., *et al.*, & James, V.H.T. (1986). A comparison of the *in vivo* uptake and metabolism of ^{3}H-oestrone and ^{3}H-oestradiol by normal breast and breast tumour tissue in postmenopausal women. *Int. J. Cancer* 38, 193–196.
9. Adams, E.F., Coldham, N.G. & James, V.H.T. (1988). Steroidal regulation of oestradiol-17β-dehydrogenase activity of the human breast cancer cell line MCF-7. *J. Endocrinol*. 118, 149–154.
10. Pasqualini, J.R., Gelly, C., Nguyen, B.-L. & Vella, C. (1989). Importance of estrogen sulfates in breast cancer. *J. Steroid Biochem.* 34, 155–163.
11. Malet, C., Vacca, A., Kuttenn, F. & Mauvais-Jarvis, P. (1991). 17β-Estradiol dehydrogenase (E2DH) activity in T47D cells. *J. Steroid Biochem. Mol. Biol.* 39, 769–775.
12. Andersson, S. (1995). Molecular genetics of androgenic 17-β-hydroxysteroid dehydrogenases. *J. Steroid Biochem. Mol. Biol.* 55, 533–534.
13. Luu-The, V., Zhang, Y., Poirier, D. & Labrie, F. (1995). Characteristics of human types 1, 2 and 3 17β-hydroxysteroid dehydrogenase activities: oxidation/reduction and inhibition. *J. Steroid Biochem. Mol. Biol.* 55, 581–587.
14. Poutanen, M., Miettinen, M. & Vihko, R. (1993). Differential estrogen substrate specificities for transiently expressed human placental 17-β-hydroxysteroid dehydrogenase and an endogenous enzyme expressed in cultured COS-m6 cells. *Endocrinology* 133, 2639–2644.
15. Labrie, F., Li, S., Labrie, C., Lévesque, C. & Mérand, Y. (1995). Inhibitory effect of a steroidal antiestrogen (EM-170) on estrone-stimulated growth of 7,12-dimethylbenz(a)anthracene (DMBA)-induced mammary carcinoma in the rat. *Breast Cancer Res. Treat*. 33, 237–244.
16. Baker, M.E. (1990). A common ancestor for human placental 17β-hydroxysteroid dehydrogenase, *Streptomyces coelicolor* actIII protein, and *Drosophila melanogaster* alcohol dehydrogenase. *FASEB J.* 4, 222–226.
17. Krozowski, Z. (1992). 11β-Hydroxysteroid dehydrogenase and the short-chain alcohol dehydrogenase (SCAD) superfamily. *Mol. Cell. Endocrinol*. 84, C25–C31.
18. Krozowski, Z. (1995). The short-chain alcohol dehydrogenase superfamily: variation on a common theme. *J. Steroid Biochem. Mol. Biol.* 51, 125–130.
19. Chen, Z., Jiang, J.C., Lin, Z.-G., Lee, W.R., Baker, M.E. & Chang, S.H. (1993). Site-specific mutagenesis of *Drosophila* alcohol dehydrogenase: evidence for involvement of tyrosine-152 and lysine-156 in catalysis. *Biochemistry* 32, 3342–3346.
20. Obeid, J. & White, P.C. (1992). Tyr179 and Lys183 are essential for enzymatic activity of 11β-hydroxysteroid dehydrogenase. *Biochem. Biophys. Res. Commun.* 188, 222–227.
21. Lin, S.X., *et al*., & Labrie, F. (1992). Subunit identity of the dimeric 17β-hydroxysteroid dehydrogenase from human placenta. *J. Biol. Chem.* 267, 16182–16187.
22. Jany, K.-D., Ulmer, W., Froschle, M. & Pfleiderer, G. (1984). Complete amino acid sequence of glucose dehydrogenase from *Bacillus megaterium*. *FEBS Lett.* 165, 6–10.
23. Froschle, M., Ulmer, W. & Jany, K.-D. (1984) Tyrosine modification of glucose dehydrogenase from *Bacillus megaterium*. Effect of tetranitromethane on the enzyme in the tetrameric and monomeric state. *Eur. J. Biochem*. 142, 533–540.
24. Ghosh, D., *et al*., & Orr, J.C. (1991). Three-dimensional structure of holo 3α,20β-hydroxysteroid dehydrogenase: a member of a short-chain dehydrogenase family. *Proc. Natl. Acad. Sci. USA* 88, 10064–10068.
25. Ghosh, D., Wawrzak, Z., Weeks, C.M., Duax, W.L. & Erman, M. (1994). The refined three-dimensional structure of 3α,20β-hydroxysteroid dehydrogenase and possible roles of the residues conserved in short-chain dehydrogenases. *Structure* 2, 629–640.
26. Ghosh, D., Erman, M., Wawrzak, C.M., Duax, W.L. & Pangborn, W. (1994). Mechanism of inhibition of 3α,20β-hydroxysteroid dehydrogenase by a licorice-derived steroidal inhibitor. *Structure* 2, 973–980.
27. Puranen, T.J., Poutanen, M.H., Peltoketo, H.E., Vihko, P.T. & Vihko, R.K. (1994). Site-directed mutagenesis of the putative active site of human 17β-hydroxysteroid dehydrogenase type 1. *Biochem. J.* 304, 289–293.
28. Murdock, G.L., Chin, C.-C., Offord, R.E., Bradshaw, R.A. & Warren, J.C. (1983). Human placental estradiol 17β-dehydrogenase. Identification of a single histidine residue affinity-labeled by both 3-bromoacetoxyestrone and 12β-bromoacetoxy-4-estrene-3,17-dione. *J. Biol. Chem*. 258, 11460–11464.
29. Murdock, G.L., Chin, C.-C. & Warren, J.C. (1986). Human placental estradiol 17β-dehydrogenase: sequence of a histidine-bearing peptide in the catalytic region. *Biochemistry* 25, 641–646.
30. Breton, R., Yang, F., Jin, J.-Z., Li, B., Labrie, F. & Lin, S.-X. (1994). Human 17β-hydroxysteroid dehydrogenase: overproduction using a baculovirus expression system and characterization. *J. Steroid Biochem. Mol. Biol.* 50, 275–282.
31. Ghosh, D., *et al*., & Lin, S.-X. (1995). Structure of human estrogenic 17β-hydroxysteroid dehydrogenase at 2.20 Å resolution. *Structure* 3, 503–513.
32. Kabsch, W. & Sander, C. (1983). Dictionary of protein secondary structure: pattern recognition of hydrogen-bonded and geometrical features. *Biopolymers* 22, 2577–2637.
33. Busetta, B. & Hospital, M. (1972). Structure cristalline et moléculaire de l'oestradiol hemihydrate. *Acta Cryst. B* 28, 1349–1351.
34. Hurley, J.H. & Dean, A.M. (1994). Structure of 3-isopropylmalate dehydrogenase in complex with NAD^+: ligand-induced loop closing and mechanism for cofactor specificity. *Structure* 2, 1007–1016.
35. Varughese, K.I., Skinner, M.M., Whiteley, J.M., Matthews, D.A. & Xuong, N.H. (1992). Crystal structure of rat liver dihydropteridine reductase. *Proc. Natl. Acad. Sci. USA* 89, 6080–6084.
36. Su, Y., Varughese, K.I., Xuong, N.H., Bray, T.L., Roche, D.J. & Whiteley, J.M. (1993). The crystallographic structure of a human dihydropteridine reductase NADH binary complex expressed in *Escherichia coli* by a cDNA constructed from its rat homologue. *J. Biol. Chem*. 268, 26836–26841.
37. Tanaka, N., Nonaka, T., Nakanishi, M., Deyashiki, Y., Hara, A. & Mitsui, Y. (1996). Crystal structure of the ternary complex of mouse lung carbonyl reductase at 1.8 Å resolution: the structural origin of coenzyme specificity in the short chain dehydrogenase/reductase family. *Structure* 4, 33–45.
38 Tunn, S., Schulze, H. & Krieg, M. (1993). 17β-hydroxysteroid oxidoreductase in epithelium and stroma of human prostate. *J. Steroid Biochem. Mol. Biol.* 46, 91–101.
39. Chen, Z., Lee, W.R. & Chang, S.H. (1991). Role of aspartic acid 38 in the cofactor specificity of *Drosophila* alcohol dehydrogenase. *Eur. J. Biochem*. 202, 263–267.
40. Zhu, D.-W., *et al*., & Lin, S.-X. (1993). Crystallization and preliminary X-ray diffraction analysis of the complex of human placental 17β-hydroxysteroid dehydrogenase with $NADP^+$. *J. Mol. Biol*. 234, 242–244.
41. Leslie, A.G.W. (1991). Molecular data processing. In *Molecular Data Processing in Crystallographic Computing*. (Moras, D., Podjarny, A.D. & Thierry, J.C., eds), pp. 50–61, Oxford University Press, UK.
42. The SERC Collaborative Computing Project, No 4. (1979). The CCP4 suite: programs for protein crystallography. Daresbury Laboratory, Warrington, UK.
43. Moy, J.P. (1994). A 200 mm input field, 5–80 keV detector based on an X-ray image intensifier and CCD camera. *Nucl. Instrum. Meth. Phys. Res. A* 348, 641–644.
44. Howard, A.J., Gilliland, G.L., Finzel, B.C., Poulos, T.L., Olhendorf, D.H. & Salemme, F.R. (1987). The use of an imaging proportional counter in macromolecular crystallography. *J. Appl. Cryst*. 20, 383–387.
45. Kabsch, W. (1988). Evaluation of a single X-ray diffraction data from a position sensitive detector. *J. Appl. Cryst*. 21, 916–924.
46. Kabsch, W. (1993). Automatic processing of rotation diffraction data from crystals of initially unknown symmetry and cell constants. *J. Appl. Cryst.* 26, 795–800.
47. Navaza, J. (1994). AMoRe: an automated package for molecular replacement. *Acta Cryst. A* 50, 157–163.
48. Brünger, A.T. (1990). X-PLOR Manual, Yale University, Newhaven, CT.
49. Jones,T.A., Zou, J.-Y., Cowan, S.W. & Kjeldgaard, M. (1991). Improved methods for building protein models in electron-density maps and the location of errors in these models. *Acta Cryst. A* 47, 110–119.
50. Jones, T.A. (1978). A graphics model building and refinement system for macromolecules. *J. Appl. Cryst.* 15, 24–31.
51. Kraulis, P.J. (1991). Molscript: a program to produce both detailed and schematic plots of protein structures. *J. Appl. Cryst.* 24, 946–950.
52. Bacon, D.J. & Anderson, W.F. (1988). A fast algorithm for rendering space-filling molecule pictures. *J. Mol. Graph.* 6, 219–220.
53. Meritt, E.A. & Murphy, M.E.P. (1994). Raster3D Version 2.0 - A program for photo realistic molecular graphics. *Acta Cryst. D* 50, 869–873.